Exponential relaxation in $TbFeO_3$: a quantum surface nucleation problem

1995 J. Phys.: Condens. Matter 7 5097

(http://iopscience.iop.org/0953-8984/7/26/015)

J. Phys.: Condens. Matter 7 (1995) 5097–5104. Printed in the UK

Exponential relaxation in $TbFeO_3$: a quantum surface nucleation problem

E B Krotenko, J Tejada and X X Zhang

Departamento Física Fonamental, Facultat de Física, Universitat de Barcelona, Diagonal 647, 08028 Barcelona, Spain

Received 6 October 1994, in final form 20 March 1995

Abstract. In this paper we present a plausible explanation for the exponential relaxation in $TbFeO_3$ single crystals observed below 3 K. Our interpretation is based on the formation and consequent propagation of the nucleated domain wall at the (010) face. The analytical calculations along the lines of current theories of macroscopic tunnelling of magnetization are in agreement with experimental results.

1. Introduction

The most interesting aspect of the behaviour of mesoscopic magnets is that at low temperature the reorientation of magnetization vector $M(r)$ occurs via quantum tunnelling between two metastable states of $M(r)$. The simplest example is the quantum underbarrier transition of the magnetic moment between easy directions in a ferromagnetic single-domain grain [1]. Similar transitions occur in quantum nucleation of magnetic bubbles [2], domain wall (DW) motion [3, 4] and the reorientation of the Néel vector in antiferromagnetic particles [5]. (For a recent review see [6]).

$TbFeO_3$ has an orthorhombically distorted perovskite structure [7]. The variety of magnetic phases observed in this material are mainly due to both the peculiarities of magnetic properties of the Tb^{3+} ion magnetism in the orthoferrite structure and the anisotropy of the exchange interaction existing between the Tb^{3+} and Fe^{3+} ions [8, 9]. In table 1 [7–9] we give information about the magnetic structure of the main magnetic phases in $TbFeO_3$ at low temperatures (between 1.7 and 10 K). Above $T = 10$ K the Néel vector in $TbFeO_3$ is parallel to the x axis. The small divergence of the magnetic moment of sublattices in $TbFeO_3$ in the y direction creates the weak ferromagnetism along the z axis. At these temperatures the Tb^{3+} ions are paramagnetic. In table 1 Γ_i, $i = 2, 4, 8$ are the irreducible representations of the space group of symmetry Pb_{nm}, to which belongs the $TbFeO_3$ single crystal; F_j and G_j are the functions symmetrical and antisymmetrical with respect to the transitions via the plane perpendicular to the j axis, C_j and A_j are the functions symmetrical or antisymmetrical with respect to the transitions via the centre of the elementary cell of $TbFeO_3$. Here $j = x, y, z$.

From the data presented it is evident that the $TbFeO_3$ single crystal at low temperatures exhibits many spin reorientations, so in order to describe the observed magnetization reversal we must determine precisely the temperature region investigated. We have a complete set of characterization data of a $TbFeO_3$ single crystal in the temperature range 1.8–300 K. Our static measurements (hysteresis loop characteristics, magnetization versus temperature) are in agreement with the proposed magnetic structure [10] and with the previous work on the

0953-8984/95/265097+08$19.50

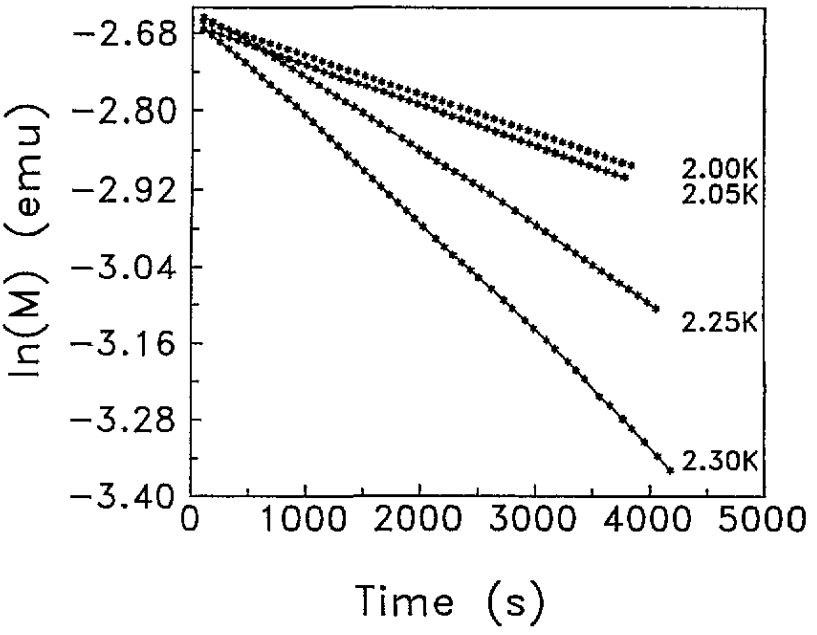

Figure 1. Magnetization relaxation data.

topic. The relaxation studies were done at $1.8 < T < 3.1$ K. In accordance with table 1, in this temperature range no substantial changes in the spin orientation in the $TbFeO_3$ single crystal are observed. At these temperatures $M \parallel Oz$ and the weak antiferromagnetic moment $l \parallel Ox$. Therefore, the interpretation of the magnetic evolution as something connected only with the thermal or quantum relaxation to some metastable state seems to be a plausible one.

The relaxation data are presented in figure 1. They follow an exponential law

$$\ln M = \ln M_0 - \Gamma t \tag{1}$$

where M_0 is the saturation magnetization and the relaxation rate Γ depends on the temperature [10].

The exponential relaxation suggests the existence of a universal single barrier U throughout the sample. Therefore, we can present Γ in the following form:

$$\Gamma = \Gamma_0 \exp[-U/k_B T^*(T)] \tag{2}$$

where Γ_0 is the attempt frequency and $T^*(T)$ is the escape temperature, which is T for thermal transitions and $T^*(T) > T$ for quantum underbarrier transitions below T_c. The latter value is defined as the crossover temperature between thermal and quantum transitions. Using the data mentioned above, it is possible to obtain U, Γ_0 and $T^*(T)$ without fitting parameters. In figure 2 we show the $T^*(T)$ data based on the results presented in [10]. From figure 2, if the magnetic field lies in the range [75; 200] Oe, T_c varies approximately from 2.2 to 2.5 K.

2. Theory

It is a well known experimental fact that at low temperatures the magnetic structure of $TbFeO_3$ consists of parallel magnetic domains separated by 180° domain walls (DWs);

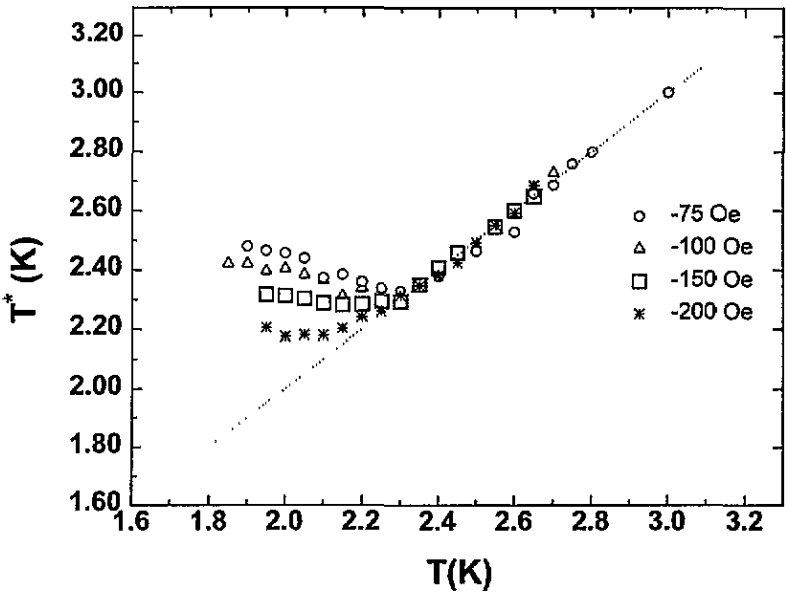

Figure 2. $T^*(T)$ data.

the theoretical interpretation of this is given in [11]. In order to explain the exponential relaxation observed we suppose that this process is connected with the growth and propagation of the DW at the crystal (010) surface (figure 3). The energy density of this DW may be written as [12]

$$W = M_0^2 w$$
$$w = -\tfrac{1}{2}\delta m^2 + \tfrac{1}{2}\alpha(\nabla l)^2 + \tfrac{1}{2}\alpha'(\nabla m)^2 + d_1 m_x l_z - d_3 m_z l_x + \beta_1 l_x^2 + \beta_3 l_z^2 \tag{3}$$

where m and l are standard vectors of ferromagnetism and antiferromagnetism, $m = (2M_0)^{-1}(M_1 + M_2)$, $l = (2M_0)^{-1}(M_1 - M_2)$, M_1 and M_2 are the magnetization vectors of superlattices, $|M_1| = |M_2| = M_0$, δ is the constant of homogeneous exchange, α and α' are the constants of non-homogeneous exchange and d_1, d_3, β_1 and β_3 are Dzialoshinskii–Moriya and anisotropy constants along x and z axes respectively. The usual minimization procedure [12, 13] gives us the DW structure corresponding to the observed Γ_4 Néel configuration:

$$\begin{aligned} &l_z = \sin\theta \qquad m_z = (d_3/\delta)\cos\theta \qquad \cos\theta = \tanh y/\Delta \\ &l_x = \cos\theta \qquad m_x = -(d_1/\delta)\sin\theta \\ &\Delta = [\alpha/(d_1^2/\delta - d_3^2/\delta + \beta_3 - \beta_1]. \end{aligned} \tag{4}$$

So the nucleated DW is situated in the xOz plane and propagates in the y direction (figure 3). From (4) one obtains

$$w = K\sin^2\theta \qquad \sigma = 4(AK)^{1/2} \tag{5}$$

where σ is the surface energy density of the DW and K is the effective anisotropy constant; following [9] we obtain $K = 1.15$ erg cm^{-3} and $A = \alpha M_0^2 \simeq 10^{-7}$ erg cm^{-1} [13], so we

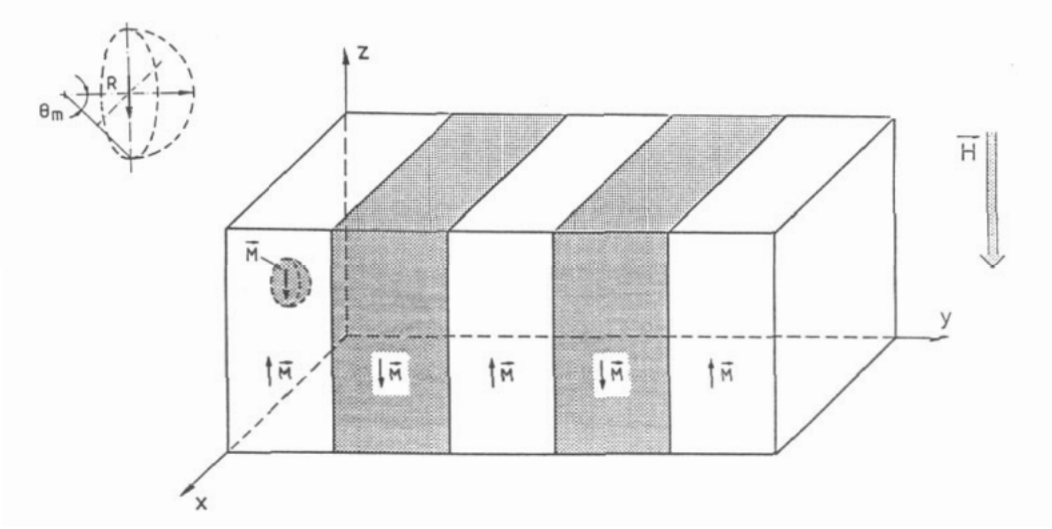

Figure 3. The geometry of the MQT process under investigation.

assume that the energy barrier caused by DW formation is

$$U = KV \tag{6}$$

where V is the volume tunnelling during one MQT (macroscopic quantum tunnelling) event. From [4, 14]

$$V = (\mu_B/\hbar)B(K\chi)^{1/2}. \tag{7}$$

Here B is the tunnelling exponent, not to exceed 30, and χ is the initial susceptibility, $\chi \simeq 10^{-4}$. Therefore, $V = 8 \times 10^4$ Å^3, so from (6) we obtain $U = 6 \times 10^{-3}$ eV in a good agreement with the value $U = (6\text{–}7) \times 10^{-3}$ eV extracted from the experimental data [10] without any fitting parameter (this possibility was pointed out before in section 1).

In order to evaluate the crossover temperature of the MQT process, we use the relation

$$k_B T_c \simeq \hbar\omega \tag{8}$$

where ω is the characteristic frequency of an instanton

$$\omega = c/\Delta. \tag{9}$$

Here c is the limiting velocity of a DW in orthoferrites (the minimal phase velocity of spin waves), which is given by [14]

$$c = \tfrac{1}{2}\gamma M_0[\alpha/\chi)^{1/2} \tag{10}$$

where γ is the gyromagnetic ratio. Therefore we obtain that

$$T_c = (\hbar\gamma/2k_B)[K/\chi]^{1/2} = (\mu_B/k_B)^{1/2}[K/\chi]^{1/2}. \tag{11}$$

This is the same expression for T_c as for the antiferromagnetic particles [4]. For the energy barrier [3]

$$U = 30k_B T_c. \tag{12}$$

Therefore, $T_c = 2.3$ K and $U = 6 \times 10^{-3}$ eV. These results are also in good agreement with the values extracted from the experimental data [10] cited before. Note that (6) and (9) are obtained independently—the first from the analysis of the static DW structure, and the second from the spin wave theory.

Following [3] the total Euclidean action of our problem may be written as

$$S_E = S_0 + S_p + S_m. \tag{13}$$

Here S_0 is the covariant action connected with the DW distortion, S_p is connected with the defects and S_m originates from the change in the Zeeman energy in the region between the nucleated DW and the (010) face (figure 3). As a good approximation [3] $|\dot{y}| \ll c$, $R \ll \Delta$, where R is the radius of curvature of the nucleated DW segment, so we obtain

$$S_0 = -\sigma_0 \int dt\, dx\, dz\, [1 + (\nabla y)^2]. \tag{14}$$

The defects are not taken into account, so for our case $S_p = 0$. In accordance with [3]

$$S_m = -\int d^4\xi M(\xi) H(\xi). \tag{15}$$

In (15) $d^4\xi = dt\, d^3R$ and the integration is over the MQT domain volume (figure 3).

We suppose that the nucleating DW has the form of a spherical segment; this seems to be so because the energy barrier in this problem is connected with DW surface nucleation, and the sphere has a minimal relation between the surface and volume. In order to describe the structure of a spherically curved DW we need to transform (4) in the following way:

$$\cos\theta = \tanh |r|/\Delta \tag{16}$$

where r is the radius vector in the yOz plane, so $r = (z^2 + y^2)^{1/2}$. In order to calculate the change of DW energy and the correction to the potential barrier we must complete the following procedure. First, we substitute the modified DW configuration of (16) into (4) and then the relations of (4) into (3) in order to obtain the DW energy density w as a function of the polar angle θ. Until this stage no difference from the previously described case of the Γ_4 Néel configuration is observed. The deviation appears during the integration

$$U = \int_v dx\, dy\, dz\, w[\theta(x, y, z)] \tag{17}$$

and it may be expressed as the modification of the surface energy density of the DW

$$\sigma_* = \sigma J$$
$$2J = \int_{-\infty}^{+\infty} \int_{-\infty}^{+\infty} \frac{dy\, dz}{\cosh^2(y^2 + z^2)^{1/2}} = \pi. \tag{18}$$

So, the deviation in the potential barrier height U caused by the spherical distortion of the DW does not exceed $\pi/2$, but due to the fact that DW segments oriented near the yOz (hard) plane have higher energy density, they will be slightly suppressed, so during the growth process the DW will change its shape and will become ellipsoidal. Consequently, factor J will become close to one.

At the last stage of the MQT process the DW has the shape of a parabolic cylinder, but the study of this goes beyond the quantum nucleation effect considered here. Note that in order of magnitude the actions computed for the distorted DW and the spherical nucleus are the same.

Following the initial hypothesis of MQT in $TbFeO_3$ with DW formation, we obtain

$$dS/dt = \text{constant} = S_t. \tag{19}$$

So the radius of the MQT region

$$R = At^{1/2} \tag{20}$$

where $A^2 = S_t/2\pi(1 - \cos\theta_m)$; here θ_m is the angle limiting the nucleus (see figure 3). In the spherical coordinate system it is possible to calculate the action (14) analytically without any additional approximations. From (15) we obtain

$$S_m = 2M_0H \int dt \int d^3R. \tag{21}$$

Finally,

$$\begin{aligned} S_0 &\simeq -2.3\sigma_0\tau^2 S_t \\ S_m &= 0.15 S_t^{3/2}\tau^{5/2} M_0 H \end{aligned} \tag{22}$$

where τ is the time of the MQT relaxation.

In order to prove that the total Euclidean action $S_E \leqslant 30\hbar$, so the tunnelling exponent $B \leqslant 30$ along the lines of MQT theory developed in [1–6], we use the relation [4]

$$B = (\gamma H_a/\omega)(h_c\epsilon)^{5/4}N. \tag{23}$$

Here H_a is the anisotropy field, from [10] $H_a \cong 6$ kOe; $h_c = H_a/H_c$, where H_c is the coercive field. Using the hysteresis loop from [10], we obtain $h_c \cong 0.2$. Note that in reality this value must be decreased substantially, because, strictly speaking, the coercive field obtained from the hysteresis loop for the bulk sample is not the same as the field to move the single DW in a practically perfect $TbFeO_3$ single crystal [13, 15]. Using the results of [15], we extract that the more realistic h_c value in (23) must be at least 3.4 times smaller, so we assume $h_c = 6 \times 10^{-2}$. Nevertheless, note that even the h_c received directly from the hysteresis loop gives us $B < 30$.

The instanton frequency $\hbar\omega = 4\pi\mu_B M_0$, and using $M_0 = 330$ G cm^{-3} [7] we obtain $\omega = 4 \times 10^{11}$ s^{-1}.

In (23) N is the number of spins tunnelling simultaneously

$$N = V_T/V_{el} \tag{24}$$

where V_T is the total tunnelling volume and V_{el} is the volume of the elementary cell of $TbFeO_3$. From [7] we extract $V_{el} = 2.3 \times 10^{-22}$ cm^3. Note that V_T is not the same as V in (6). Really, in order to evaluate the energy barrier connected with the DW formation following (6), we need only the volume of a new DW; this value was evaluated in [14]. In (24) $V_T \gg V$ is the total tunnelling volume containing the DW and the domain inside it. To find V_T we need the critical radius of the nucleus, which we extract from the condition

$$E_w = E_Z. \tag{25}$$

Here E_w is the DW energy and E_Z is the Zeeman energy of the domain. Taking into account that the MQT region has the form of a spherical segment, we obtain

$$R = 3\sigma/M_0H(1-\cos\theta_m)(2+\cos\theta_m). \tag{26}$$

In order to obtain θ_m (the critical angle that limits the MQT region) we need the minimum of $R(\theta_m)$ (to realize the MQT process in a smaller region, i.e. to make it easier). This seems to be so due to the general fact connected with the principle of minimal action, because we want to provide the optimal form of a spherical segment with a minimized relation between the surface and the volume. Indeed, in general the MQT theory is also based on the procedure of minimization of action.

Finally, we find

$$\cos\theta_m = -\tfrac{1}{2} \tag{27}$$

and the critical size $R_0 \simeq 1.7 \times 10^{-5}$ cm. Taking into account that

$$V_T = \pi R^3(1-\cos\theta_m)^2(2+\cos\theta_m)/3 \tag{28}$$

we obtain $N = 7.8 \times 10^7$. Here we will assume $\epsilon = 10^{-4}$ [4]. This means that the demagnetizing field outside the sample is close to the anisotropy field. This suggestion seems to be logical because the slow stage of the relaxation studied by us as well as the MQT nucleus formation is initiated when the barrier for the wall to enter the sample just starts to develop. Really, this means that the magnetic system investigated is in the critical state.

Finally,

$$B \cong 5 < 30. \tag{29}$$

Table 1. The spin configurations corresponding to the main (non-angular) low-temperature magnetic phases in $TbFeO_3$.

Fe^{3+}	0–3.1 K Γ_4 $(G_xA_xF_z)$	3.1–10 K Γ_2 $(F_xC_yG_z)$	> 10 K Γ_4 $(G_xA_yF_z)$
Tb^{3+}	0–3.3 K Γ_8 (A_xG_y)	3.3–8.4 K Γ_2 (F_xC_y)	> 8.4 K Γ_8 (A_xG_y)

3. Conclusions

The MQT theory presented is in good agreement with experimental data. Indeed, the potential barrier values deduced theoretically ($U = 6\times10^{-3}$ eV if we assume $U = KV$ or $U = k_BT_c$) correspond to the value extracted from the experimental data, U =(6–7)$\times10^{-3}$ eV. The temperature of the transition between 'classical' thermal activated and quantum regimes of relaxation, obtained theoretically as $T_c = 2.3$ K, is the same as the experimental value $T_c = 2.2$–2.5 K.

We thus give a plausible explanation of the experimental fact that the MQT process in $TbFeO_3$ exhibits a single energy barrier. Really, the value $U = KV$, where V is determined from [4, 9] and is fixed throughout the relaxation process.

We suppose that the observable deviation from the exponential relaxation law in figure 1 may be connected with the relaxation process via other (substantially lower) potential barriers occurring in a $TbFeO_3$ single crystal in the temperature region under investigation. Naturally, the DWs in $TbFeO_3$ may pin on the lead impurities which have entered the crystal during its growth [16, 17]. Another potential barrier may be connected with the creating of new structural elements of DWs (Bloch lines, Bloch points) as well as with the change of the DW structure of Bloch type described by (4) into an intermediate one (with the deviation of vector M from the DW plane [18]). All these changes in the DW structure lead to the increase of the effective wall mass and, consequently, create an additional potential barrier [19, 20]. The processes mentioned above are connected, because the DW pinning on the defect points may promote the appearance of Bloch lines or Bloch points [13].

Nevertheless, these processes alone cannot explain the relaxation data observed. Therefore, it does not seem that our theory has an internal logical contradiction, or any contradiction with experimental data or with previous work in MQT theory [1–6]. We may suppose that the MQT process observed in $TbFeO_3$, which demonstrates the exponential relaxation law and the single energy barrier, is caused by DW formation and the consequent movement from the $TbFeO_3$ surface into the core.

Acknowledgment

This work has been supported by a NATO grant (EK).

References

[1] Chudnovsky E M and Gunter L 1988 *Phys. Rev. Lett.* **60** 661
[2] Chudnovsky E M and Gunter L 1988 *Phys. Rev.* B **37** 9455
[3] Stamp P C E 1991 *Phys. Rev. Lett.* **66** 2802
[4] Chudnovsky E M, Iglesisas O and Stamp P C E 1992 *Phys. Rev.* B **46** 5392
[5] Barbara B and Chudnovsky E M 1990 *Phys. Rev.* A **145** 205
[6] Chudnovsky E M 1993 *J. Appl. Phys.* **73** 6697
[7] Bertaut E F, Chappert J, Mareschal J, Rebouillat J P and Sivardiere J 1967 *Solid State Commun.* **5** 293
[8] Belov K P, Zvezdin A K and Mukhin A A 1979 *Sov. Phys.–JETP* **49** 557
[9] Derkachenko V N, Zvezdin A K, Krinetskii I B, Kadomtseva A M, Mukhin A A and Khokhlov V A 1980 *Sov. Phys.–Solid State* **22** 1021
[10] Zhang X X, Tejada J, Roig A, Nikolov O and Molins E 1994 *J. Magn. Magn. Mater.* **137** L235
[11] Farztdinov M M, Shamsutdinov M A and Khalfina A A 1979 *Sov. Phys.–Solid State* **21** 878
[12] Turov E A 1953 *Physical Properties of Magnetically Ordered Crystals* (Moscow: USSR Academy of Sciences)
[13] Malozemoff A P and Slonzewski J C 1979 *Magnetic Domain Walls in Bubble Films* (New York: Academic)
[14] Chudnovsky E M 1994 unpublished
[15] Krotenko E B, Kuzin Yu A, Melikhov Yu V, Redchenko A M and Baryakhtar F G 1995 *J. Magn. Magn. Mater.* at press
[16] Bidaux R, Bouree J E and Hammann J 1975 *J. Physique* **36** 803
[17] Bouree J E and Hammann J 1975 *J. Physique* **36** 391
[18] Khodenkov G E 1985 *Sov. Phys.–Solid State* **27** 334
[19] Krotenko E B, Kuzin Yu A, Melikhov Yu V, Redchenko A M and Baryakhtar F G 1994 *J. Magn. Magn. Mater.* **136** 59
[20] Grishin A M and Krotenko E B 1994 unpublished